DOI: 10.61782/fa.2023.0243

FLUTIST ROBOT, AN ENVIRONMENT TO EXPERIMENT WITH FLUTE ACOUSTICS

F. Hurtado[1*] **P. de la Cuadra**[1] **M. A. Torres**[1] **B. Fabre**[2]
[1] Departamento de Ingeniería Eléctrica, Escuela de Ingeniería, Pontificia Universidad Católica de Chile, Chile
[2] Institut Jean Le Rond d'Alembert, Sorbonne Université, France

ABSTRACT

Recent studies on flute-like instruments have raised interest in creating an environment to precisely control and measure the strategies used by flutists while controlling their instruments. A robotic setup is proposed. Capable of independently controlling the three parameters that are crucial to producing a musical sound from the instrument: (1) the length of the air jet l, (2) its angle into the flute θ, (3) the jet's offset with respect to the labium of. It also allows for precise control of the jet speed u_j and the trajectories for every parameter. A custom-designed artificial mouth can move around a fixed flute by a three-axis mechanism operated with stepper motors. The air jet velocity is controlled with a mass flow controller connected to an air compressor. Another robotic mechanism is proposed to emulate the fingerings acting on the keys, creating a versatile testbed to study the musician's control dynamically. Both, the details of the mechanical design and the future possibilities of the robot will be discussed. We strongly believe that the robot will let us validate many aspects of our knowledge of flute acoustics, understand the details of the instrument design and improve our understanding of the complex relationship between the flutist and its instrument.

Keywords: *Acoustic Robotics, Robot Design, Flute Control Strategies, Flute-like Instruments, Musical Acoustics*

*_**Corresponding author**_: *fernandohurtado@uc.cl.*

1. INTRODUCTION

The understanding of the sound mechanism of flute-like instruments has made significant progress since research began in the last century. Multiple authors have contributed to this field, leading to advancements in areas such as flute acoustics, physical modeling, and design. However, the precise interpretation of the interaction between the musician and the instrument remains unclear [1]. With this motivation, Ernoult & de la Cuadra [2] sought to measure and model the effect on the impedance of the musician's face while playing, and thus propose a tuning profile method that, takes into account this parameter. Their study raised several questions about the musician's control gesture and its connection to the instrument's geometry, offering prospects to supplement the current model. However, conducting experiments to explore these questions requires precise control of specific parameters and the ability to replicate conditions. Thus, the idea of a robotic set-up emerged - an interactive and configurable set-up that would allow for the conduction of various experiments in the research of these questions.

Since the early days of studying flute acoustics, ingenious machines have been developed to aid in the process. For instance, in 1968, Coltman created an artificial air supply that could emulate a player's lips. He then used this apparatus to blow a head joint and measure its acoustic impedance at different values of inlet pressure and lip-to-edge distances [3]. Similarly, in 1970, Ando proposed a configurable mechanical apparatus capable of setting the four primary aeroacoustic parameters, with which he could estimate the ranges of these parameters [4]. Sawada and Sakaba built an artificial blowing device in 1980 to study the effects of various factors, such as the speed of the blowing air jet, the attack angle, the lip-to-edge distance, and the transverse displacement of the jet, on the transition in the sounding mode [5]. More recently, in 2010, Ferrand developed a controlled system that could precisely manipulate the pressure inside an artificial mouth cavity. This system was used to study recorders [6]. Auvray proposed an interesting experimental setup in 2016 to study the aeroacoustic properties of panpipes. He was able to manually control the jet-pipe angle and the jet velocity with a mass flow controller [7]. In 2021, Onogi used a displaceable artificial mouth to study the effects of the primary aerodynamic parameters on the harmonic composition of radiated sound in a flute [8].

The development of the Waseda Flutist Robot, WF-4RV, by Solis at the University of Waseda in Japan [9], also served as a significant inspiration for this project. This impressive anthropomorphic robot, with 41 degrees of freedom, was designed to play music with a transverse flute using a mechanism similar to that of humans. Its primary focus was on the interaction between humans and robots, understanding human motor control, generating artistic performances, and educating players of the flute. While it has not been used for experiments related to flute acoustics, its mechanism and experience offer valuable insights for our project.

2. METHODOLOGY

2.1 Early prototypes and learnings

The robotic solution was developed iteratively, beginning with a focus on achieving correct control over the flow in the first iteration. During this phase, the selection of the mass flow controller was discussed, including its requirements in terms of precision, range, and communication protocol with the computer. The first prototype was completed with the necessary drivers and a GUI featuring real-time plots and the ability to set different signals as a reference to the control loop.

Then a three-axis mechanism to mount an artificial mouth connected to the flow system was included. This three degrees of freedom (DOF) mechanism was discussed and modeled until a satisfactory solution was found. NEMA 23 Stepper motors were selected to move each axis and were initially controlled in an open-loop system. Ten different prototypes were built for the artificial mouth design, and each prototype revealed an aspect to improve for the next iteration showing how hard it is even to produce a simple sound from a flute. Thus, the first blowing and moving prototype was built.

Finally, the three-axis mechanism was improved by replacing the drivers of the steppers with three AMCI-D4840E2 that included new functionalities, such as the option to couple encoders, reading of position in real-time, and the usage of the same communication protocol as the mass flow controller. Encoders were later added to the motors, and the control system was replaced with a closed-loop strategy.

Then the fingers' action was considered. The first attempt to tackle the problem involved using a mechanism with levers and elastic bands to press each different key, and servo motors were used to raise the levers again. It was soon replaced by a more manageable system that allowed better handling of the instrument and had more torque in the motors to close the gaps that were sometimes left open in the keys. This solution also improved the synchronism in the keys' movements and allowed faster transitions.

2.2 Current design

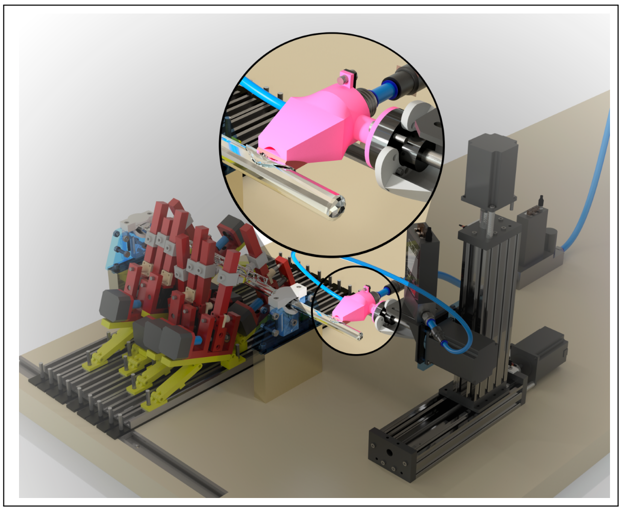

Figure 1: A render of the final design with a zoom-in to the artificial mouth in position with the flute

The current design aims to control the variables that affect most significantly the sound produced by the flute. The length of the air jet l and the air jet speed u_j determine the reduced jet velocity which is considered a good descriptor of the state of the system [10]. The incident angle θ and the offset of the jet of affect the harmonic structure [8] and in the window impedance [2]. Also, these four parameters have been controlled in other experiments before [4,5,8,11]. Parameters like the lips configuration and the lower lip geometry are only secondary parameters and therefore are not addressed with this version of the robot.

The design will be explained in three parts, first, the three-axis mechanism will be discussed, then the flow control system, and finally the fingers solution.

2.2.1 *Three axis mechanism*

A 3-DOF system for the mouth position was chosen to provide control over the three positional variables: the length of the jet, its angle of incidence on the labium, and its offset. These variables are defined as seen in figure 2. The desired motion however is accomplished with a rotational axis (from now called α) mounted on an XZ cartesian robot as seen in figure 3. As each axis is not straightly related to one of the variables used to describe the mouth position with respect to the flute, a conversion between the two systems is necessary: the joints space system (X, Z, and α), and the task space system (l, θ and of).

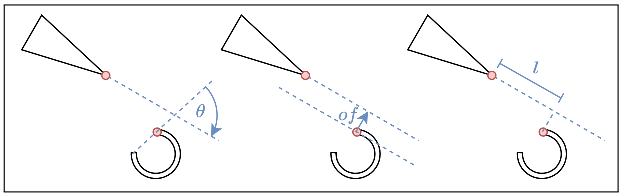

Figure 2: Definition of the incidence angle (θ), the offset of the jet (o) and its length (l) where the triangle represents the mouth and the circle a transversal cut of the flute with the red dots indicating the lips and the labium

The origin of the joint system is defined at the limits of axes X, Z when their motors are rotated counterclockwise. The rotational axis has its origin -where the angle is 0- at the position where the artificial mouth is oriented to match $+\hat{x}$. Both the origins for X, Z, and α are found at the homing routine, which is performed every time the robot starts.

The position of the lips of the artificial mouth, which is the place where the jet detaches from the mouth, is defined as (x', z'), and is calculated considering the distances of the motor mounting displacement and the artificial mouth geometry. It is important to know the location of this point because it is from here that l, θ, and of are measured.

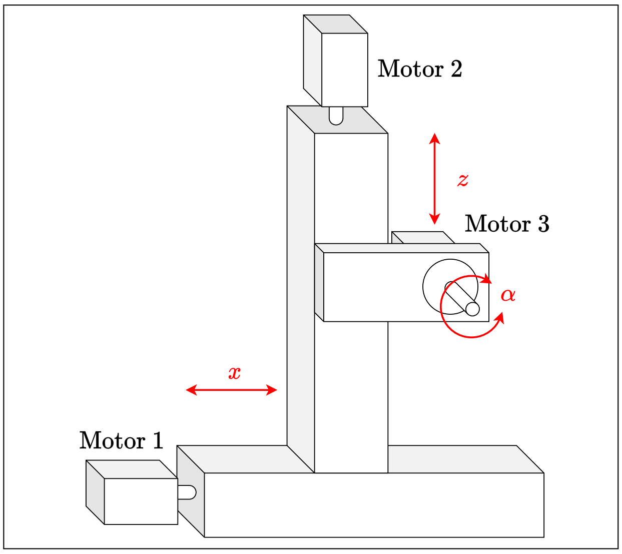

Figure 3: Three-axis mechanism to control the position of the mouth

The flute is firmly fixed in a constant position (x_f, z_f) (location of the tips of the labium in the joint space system), and α_f the inclination of the window opening with respect to the horizontal. The conversion from the joint space system to the task space system is as follows:

$$\begin{pmatrix} x' \\ z' \end{pmatrix} = \begin{pmatrix} x \\ z \end{pmatrix} + \begin{pmatrix} d_h \\ d_v \end{pmatrix} \begin{bmatrix} \cos\alpha & -\sin\alpha \\ \sin\alpha & \cos\alpha \end{bmatrix} \quad (1)$$

$$\begin{pmatrix} l \\ of \end{pmatrix} = \begin{pmatrix} x' - x_f \\ z' - z_f \end{pmatrix} \begin{bmatrix} -\cos(\alpha) & -\sin(\alpha) \\ \sin(\alpha) & -\cos(\alpha) \end{bmatrix} \quad (2)$$

$$\theta = \alpha + \alpha_f \quad (3)$$

The path for a certain movement can be defined in several ways, and it depends on the application which works better. The most simple method to define it is through straight lines, either in the space of the joints or the task [12]. As one of the purposes is to evaluate the effects of l, θ, of on the produced sound, and ramps on each of these variables without changing the others are seek, the path planning strategy followed by the robot is using straight lines in the space of the task. Then, once the path is defined, a time scaling algorithm is performed to relate a desired position to a certain time, so that the velocities

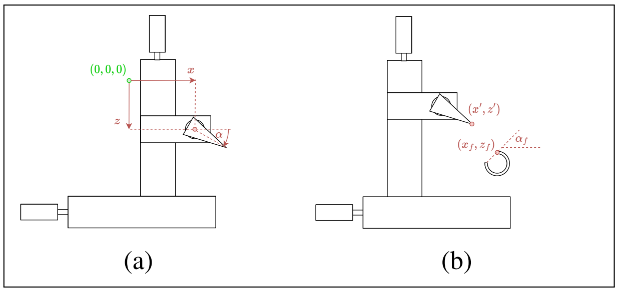

Figure 4: (a) Shows the joint space measurement system and (b) the mouth end and flute position

and accelerations required in each motor are within the ranges of the robot. Finally, this path is traduced to the task space system, and it can be communicated. With this information the table 1 is built and used as a road guide.

Table 1: Trajectory planning strategy

Time	Task coordinates	Joint coordinates
t_0	(l_0, θ_0, of_0)	(x_0, z_0, α_0)
t_1	(l_1, θ_1, of_1)	(x_1, z_1, α_1)
$\vdots$	$\vdots$	$\vdots$
t_n	(l_n, θ_n, of_n)	(x_n, z_n, α_n)

To transform from the task coordinates to the space of the joints, equations 1, 2 and 3 are inverted.

Each motor is controlled with an SD4840E2 Networked Stepper Indexer/Driver, which communicates with the PC controller via Ethernet/IP to synchronize the motion. The desired position and speed for each axis are reported to the corresponding driver every 10ms which then drives the motor taking into consideration the acceleration and deceleration limits. Encoder feedback is read by the PC controller to have a more reliable measure of the position, which could be different to expected due to step loss in the stepper motors. This is finally corrected with an integrative controller.

2.2.2 Flow control

The air coming out from the compressor is regulated to feed a mass flow controller with regular 20 PSI pressure on its inlet. The mass flow controller used is the Alicat MCP-50SLPM-D-EIP, which is designed to provide a controlled airflow within the range 0-50 SLPM (standard liters per minute) with a precision of $\pm$ (0.8% of reading + 0.2% of full scale). It has a PID controller integrated and is connected to the main computer using Ethernet/IP. Every 10ms the flow readings are informed to the computer and the reference for the desired flow is sent to the controller. The outlet of the mass flow controller is connected to a custom-designed artificial mouth, where the internal pressure is measured for reference. This setup is presented in figure 5.

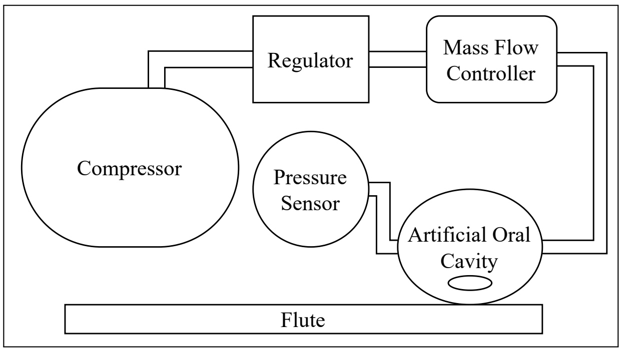

Figure 5: General set-up for the controlled air supply

The artificial mouth was designed to resemble the musician's mouth when performing music with a flute. It has an inner volume of approximated 21.5 cm^3, the lips are shaped to have a surface of approximated 29 mm^2, a height of 3.5 mm and a width of 13 mm. Future works consider the possibility of changing its shape dynamically, but for now is fixed on a shape that delivered well sounding for both low and high registers. The mouth has attached a soft piece on its bottom to act as a lower lip and maintain the contact with the flute in every moment. The artificial mouth, along with the soft piece that is attached to it are represented in figure 6.

2.2.3 Fingering solution

A low-cost robotic solution that can emulate finger action was implemented. It can be customized to meet different needs. Figure 7 illustrates one actuator, which is responsible for activating a single key and is mounted on an adjustable platform. This platform enables users to adjust the angle, radial distance, and position along the flute to accommodate various flute geometries. Nine of these actuators were built, each designed with a range of movement of 4mm, which can be traveled in less than 100ms with sufficient torque to press the key.

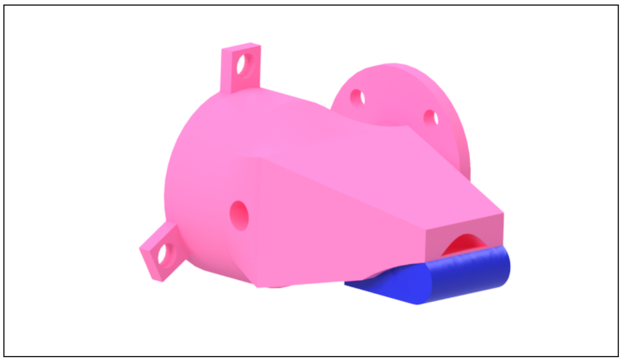

Figure 6: Artificial mouth in pink with the soft piece that acts as the lower lip in blue

Each one of these actuators is independently controlled by an Attiny Arduino, which is connected to a main Arduino board, which in turn is connected to a computer that issues commands. We made this decision to improve the scalability of the system without compromising its computational efficiency, which could otherwise slow down the actuators' response time.

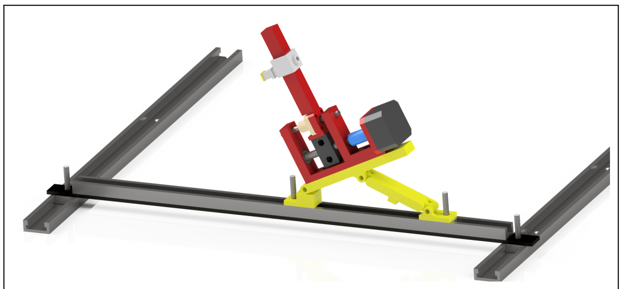

Figure 7: Finger actuator mounted on rails

3. EXPERIMENTS

Two experiments were proposed. In the first, step references were given to each axis and the flow system to measure their responses. For this experiment, each axis was measured while the others were not moving. The references for the position and velocity were reported to the corresponding drivers every 10ms, and the acquisition of data every 50 ms. For the X and Z axes, a 10mm step was given as reference, to the α axis a 15° step and to the flow controller a 20 SLMP step. The three-axis PID control loops were tuned heuristically, and the mass flow controller was tuned by its manufacturer. This experiment gives us information on the stability of the system along with its capacity to reach a stationary state.

In the second experiment, the robot was challenged to perform a chromatic scale from D3 ($\approx$ 294 Hz) to A5 ($\approx$ 1760 Hz) with every note having the same duration of 2 seconds. Its response was measured by a microphone 20 cm from the labium. For this experiment, a dictionary with the set points for every note was built manually considering De la Cuadra's measurements as a starting point [13]. Figure 8 shows the obtained dictionary.

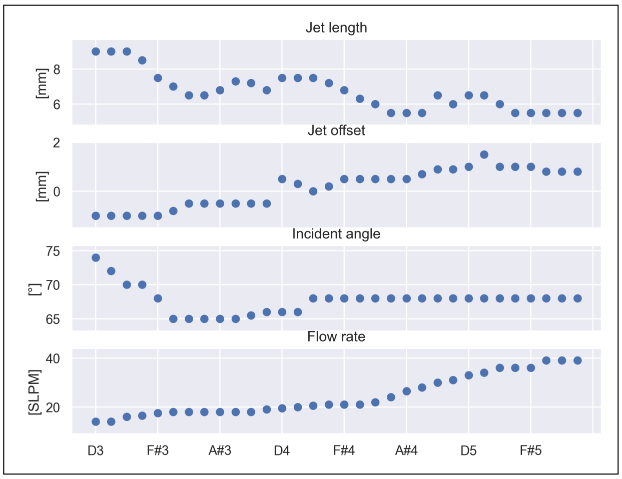

Figure 8: Dictionary created to play the scale

4. RESULTS

All the step responses are plotted in figure 9. The rise time, overshoot, and settling time for each axis are tabulated in table 2. Here, similar responses are seen for axes X and Z, which was expected since they perform similar tasks; however, they manage different loads. The axis α shows the largest overshoot, which could be explained by the lower stroke of the motor required for the job. The flow shows the fastest response time, but it must be considered that the other systems deal with higher inertia and have limited acceleration. The flow also shows a difference at zero reference, that is due to a leakage of air, which, although undesirable, is unable to start an oscillation in the flute. All the systems show stable responses and times within the accepted margins. It is important to note that as the complete system is still under development, this does not represent a final result, but a demon-

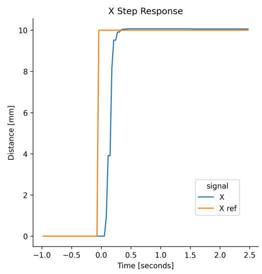

(a) X Step Response

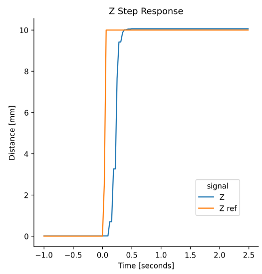

(b) Z Step Response

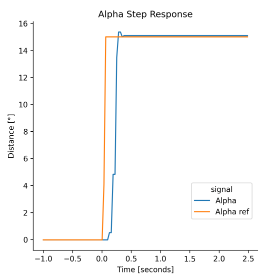

(c) α Step Response

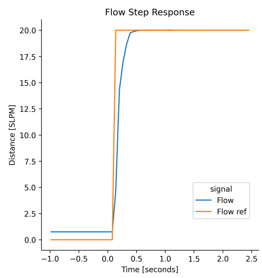

(d) Flow Step Response

Figure 9: Step response of each system

stration of the system's capabilities and that it can still be tuned to adapt to different needs.

Table 2: Step response characteristics for each axis

	Rise time	Overshoot	Settling time
X	0.063s	0.099%	0.243s
Z	0.061s	0%	0.313s
α	0.062s	1.789%	0.253s
Flow	0.125s	0.083%	0.329s

The chromatic scale performed was recorded and analyzed using the Signal package provided by Scipy in Python. Its spectrogram is plotted in figure 10, where its harmonic structure is presented. In figure 11 the fundamental frequency for each note was calculated using the pYIN algorithm [14] and their detuning was plotted in cents. In this last figure is possible to recognize that the robot was able to play all the notes in the register. While the lower notes show a detuning towards a lower pitch, the higher notes a detuning towards a higher pitch. The lower notes also show a more distributed energy along the harmonics, while higher notes show a very predominant fundamental. These differences can be explained by the selection of the parameters, which were selected by prioritizing the timbre over the correct pitch. Overall, the complete range shows concordance between desired and obtained sounds and up to five harmonics are observed in the most timbred notes.

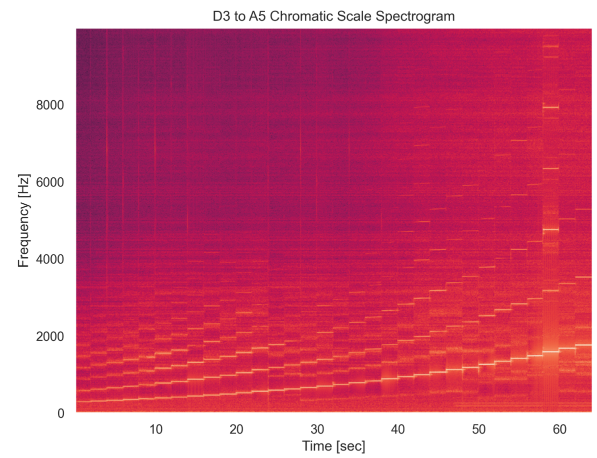

Figure 10: Spectrogram of the chromatic scaled performed by the robot

5. CONCLUSIONS

The robotic system shows acceptable accuracy in terms of motion and sound produced. The experiments realized suggests that the current version of the robot is promising and already available for restricted experimentation. Fine adjustments are still necessary to improve the control and future versions should consider a more dedicated analysis to the selection of its parameters.

The potential applications of this robot in the field of studying physical modeling of flutes, instrument design, flute education, and creative composition are vast. Its versatility makes it an invaluable tool in various research areas.

One area where this robot shines is in the analysis of expert flutist techniques. By being able to play the flute with a robot, we gain valuable insights into the flutist's expertise and manipulation of the instrument. This opens up new avenues for understanding the intricate nuances of flute performance.

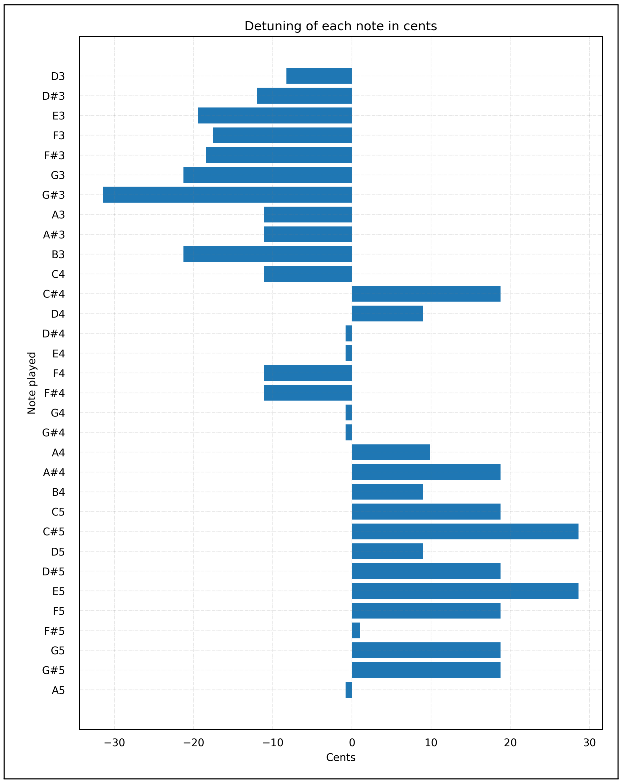

Figure 11: Detuning of each note played in the chromatic scale

6. REFERENCES

[1] A. Chaigne, J. Kergomard, and B. Fabre, *Flute-Like Instruments*, pp. 559–606. Springer New York, 05 2016.

[2] A. Ernoult, P. de La Cuadra, and B. Fabre, "An Inclined Plane: A Simple Model for the Acoustic Influence of the Flutist's Face," *Acta Acustica united with Acustica*, vol. 104, pp. 496–508, 05 2018.

[3] J. W. Coltman, "Sounding mechanism of the flute and organ pipe," *The Journal of the Acoustical Society of America*, vol. 44, pp. 983–992, Oct. 1968.

[4] Y. Ando, "Drive conditions of a flute and their influences upon sound pressure level and fundamental frequency of generated tone: An experimental study of a flute i," *THE JOURNAL OF THE ACOUSTICAL SOCIETY OF JAPAN*, vol. 26, no. 6, pp. 253–260, 1970.

[5] Y. Sawada and S. Sakaba, "On the transition between the sounding modes of a flute," *The Journal of the Acoustical Society of America*, vol. 67, pp. 1790–1794, May 1980.

[6] D. Ferrand, C. Vergez, B. Fabre, and F. Blanc, "High-precision regulation of a pressure controlled artificial mouth : the case of recorder-like musical instruments," *Acta Acustica united with Acustica*, vol. 96, no. 4, pp. 701–712, 2010.

[7] R. Auvray, B. Fabre, F. Meneses, P. de la Cuadra, and P.-Y. Lagrée, "Specific features of a stopped pipe blown by a turbulent jet: Aeroacoustics of the panpipes," *The Journal of the Acoustical Society of America*, vol. 139, pp. 3214–3225, June 2016.

[8] K. Onogi, H. Yokoyama, and A. Iida, "Effects of jet angle on harmonic structure of sound radiating from the flute," *Acta Acustica*, vol. 5, p. 11, 2021.

[9] J. Solis, K. Taniguchi, T. Ninomiya, T. Yamamoto, and A. Takanishi, "Refining the flute sound production of the waseda flutist robot the mechanical design of the artificial organs involved during the flute playing," *Mechanism and Machine Theory*, vol. 44, no. 3, pp. 527–540, 2009. Special Issue on Bio-Inspired Mechanism Engineering.

[10] F. Blanc, B. Fabre, N. Montgermont, P. D. L. Cuadra, and A. Almeida, "Scaling of flute-like instruments: An analysis from the point of view of the hydrodynamic instability of the jet," *Acta Acustica united with Acustica*, vol. 96, pp. 642–653, July 2010.

[11] P. de La Cuadra, *The sound of oscillating air jets: Physics, modeling and simulation in flute-like instruments*. PhD thesis, Stanford University, California, Jan. 2006.

[12] K. M. Lynch and F. C. Park, *Modern Robotics: Mechanics, Planning, and Control*. USA: Cambridge University Press, 1st ed., 2017.

[13] P. de la Cuadra, B. Fabre, N. Montgermont, and C. Chafe, "Analysis of flute control parameters: A comparison between a novice and an experienced flautist," *Acta Acustica united with Acustica*, vol. 94, pp. 740–749, Sept. 2008.

[14] M. Mauch and S. Dixon, "Pyin: A fundamental frequency estimator using probabilistic threshold distributions," in *2014 IEEE International Conference on Acoustics, Speech and Signal Processing (ICASSP)*, pp. 659–663, 2014.